Accepted Manuscript

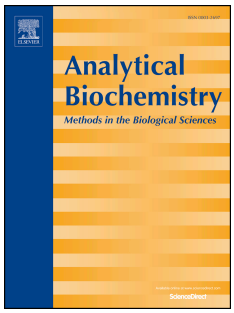

Application of nanomaterials for the electrical and optical detection of the hepatitis B virus

Danielle A. Oliveira, Jussara V. Silva, José M.R. Flauzino, Ana C.H. Castro, Anna C.R. Moço, Márcia M.C.N. Soares, João M. Madurro, Ana G. Brito-Madurro

PII: S0003-2697(18)30319-1

DOI: 10.1016/j.ab.2018.03.023

Reference: YABIO 12976

To appear in: *Analytical Biochemistry*

Received Date: 10 December 2017

Revised Date: 24 March 2018

Accepted Date: 25 March 2018

Please cite this article as: D.A. Oliveira, J.V. Silva, José.M.R. Flauzino, A.C.H. Castro, A.C.R. Moço, Má.M.C.N. Soares, Joã.M. Madurro, A.G. Brito-Madurro, Application of nanomaterials for the electrical and optical detection of the hepatitis B virus, *Analytical Biochemistry* (2018), doi: 10.1016/j.ab.2018.03.023.

APPLICATION OF NANOMATERIALS FOR THE ELECTRICAL AND OPTICAL DETECTION OF THE HEPATITIS B VIRUS

Danielle A. Oliveira[a], Jussara V. Silva[b], José M. R. Flauzino[a], Ana C. H. Castro[a], Anna C. R. Moço[a], Márcia M. C. N. Soares[c], João M. Madurro[b], Ana G. Brito-Madurro[a]*

a. Institute of Genetics and Biochemistry, Federal University of Uberlândia, Uberlândia, Brazil

b. Institute of Chemistry, Federal University of Uberlândia, Uberlândia, Brazil

c. Adolfo Lutz Institute, Regional Laboratory in São José do Rio Preto, Brazil

*Author to whom correspondence should be addressed: Tel. +55 34 32182203; Fax: +55 3432182203; E-mail: agbrito@ufu.br

Abstract

This work describes different approaches for the detection of hepatitis B virus (HBV) genomic DNA, using electrochemical and optical techniques. The platforms consisted of a single-stranded DNA probe (HEPB1S), specific to HBV, grafted on a gold electrode modified with reduced graphene oxide or gold nanoparticles. Differential pulse voltammetry analysis indicates that the addition of HBV genomic DNA caused an increase of about 1.4 times in the current peak value, when compared to the negative control. It was observed a linear dependence with the log HBV-genomic DNA concentration and the electrochemical biosensor detected until 7.65 $pg.\mu L^{-1}$ of the target. Electrochemical impedance spectroscopy measurements showed an increase of about 2 times in the charge transfer resistance, after the addition of HBV genomic DNA. Assays using colloidal suspension of gold nanoparticles showed a shift of the peak wavelength, linearly proportional to the HBV-genomic DNA concentration, with a detection limit of 0.15 $ng.\mu L^{-1}$. The applicability of the gold nanoparticles for clinical samples was tested with success in the blood plasma. All the approaches used in this work were effective in detecting genomic DNA or blood plasma in positive samples for HBV.

Keywords: hepatitis B; genosensor; electrochemical detection; gold nanoparticles

1 Introduction

Over the past few decades, nanomaterials based on carbon and noble metals, such as reduced graphene oxide (rGO) and gold nanoparticles (AuNPs) have gained space in scientific research due to their distinct properties, such as high electrical and thermal conductivities, surface-to-volume ratio, electron mobility at room temperature, a high mechanical resistance and large surface area [1-4].

These materials are widely employed to increase the performance of DNA biosensors [5,6] combining their excellent properties with the stability and complementarity of the DNA molecules using an electron transfer reaction through π-stacked DNA duplex, electroactive tags or intercalators [7-9].

The demand for optical and electrical biosensors has grown as alternatives to the current methods, since they can be used as real-time diagnostic devices, requiring no professional handling, with a quick response and relatively low cost of construction, are potentially miniaturized and portable. Recent advances in micro and nanotechnologies have allowed the development of highly sensitive and cost-effective electrochemical and optical biosensors [10] for hepatitis B virus detection [11].

Hepatitis B is a disease caused by a viral infection in liver cells and occurs through percutaneous and mucosal membrane exposure to contaminated blood and body fluids, including serum, semen and saliva [12]. It can be asymptomatic, rapid and progressive, and remains as a great public health problem [13-15]. The World Health Organization estimates that there are 240 million people chronically infected with hepatitis B virus (HBV) in the world, with about 600,000 deaths per year [16]. Complete vaccination is the most effective strategy to reduce global morbidity and mortality [17]. However, there is a portion of individuals who do not respond positively to this immunization. There are several tests for the HBV detection, for the disease progression monitoring, and to check the acquired immunity, such as the immunoenzymatic assay (ELISA), Western Blot, fluoroimunoassay, and polymerase chain reaction [13, 14]. However, these techniques require the use of expensive equipment and reagents as well as skilled personnel, and are performed exclusively in a hospital or laboratorial environment [18]. Genosensors that do not need an amplification step are of greater interest for public health simplifying and reducing the assay time [11], where the electrochemical methods allows the combination of the especifity of biological identification with the selectivity of physicochemical transduction on the hybridization event [19].

The electrochemical or optical behavior of DNA aiming the biosensor construction for hepatitis B have been investigated. Chen and collaborators [20] development a nanostructured impedance biosensor with two dynamic linear ranges, 102–103 and 103–105.1 copies/mL, and detection limit of 111 copies/mL. Ahangar and Mehrgardi developed electrochemical DNA biosensor for detection of Hepatitis B virus [21] using ferrocene as a redox reporter. The dynamic range was from 0.4 to 10 nmol of target with detection limit of 10 pmol. Mashhadizadeh *et al.* [16] grafited thiol modified Hepatitis B virus (HBV) probe DNA onto magnetite and gold nanoparticle modified carbon paste electrode. The sensing platform integrated two nanoparticles presented linear range of about 8.3×10^{-13} to 6.4×10^{-7} M and detection limit of 3.1 $(\pm0.1)\times10^{-13}$ M. Mao *et al.* reported a colorimetric detection method of hepatitis B virus DNA based on DNA-templated copper nanoclusters with a detection limit of 12×10^{9} molecules [22].

Mostly of current genossensors for hepatites B diagnosis in the literature are based on the detection of amplifed polimerase chain reaction (PCR) fragments [23-25], thus introducing an additional step in the process, which is laborous and costly.

In this context, electrical and optical methods were used in this work for the detection of the genomic DNA from blood plasma of patients with hepatitis B, with no PCR amplification (Fig. 1). This is a new platform using a specific probe for the genomic DNA of the HBV onto gold electrodes modified with reduced graphene oxide or gold nanoparticles.

Here Figure 1

2 Experimental

2.1 Chemicals and solutions

All reagents were of analytical grade, without previous purification. Ultra high purity water (18.2 MΩ.cm, Master System, Gehaka, Brazil) was used for the preparation of all solutions. Ethidium bromide (3,8-diamino-5-ethyl-6-phenyl phenatridinium bromide) was obtained from Merck KGaA. All solutions used in the electrochemical analysis were deoxygenated by means of ultra-pure nitrogen bubbling for at least 25 minutes before use. Tetrachloroauric (III) acid trihydrate (99%), graphite powder,

potassium permanganate ($KMnO_4$) and sulfuric acid (H_2SO_4) were purchased from Sigma-Aldrich Chemical, USA (ACS purity). Ammonium hydroxide 28% (w/v) and sodium nitrate were purchased from Synth. The DNA oligonucleotide probe for the HBV virus (HEPB1S) was synthesized by Invitrogen Life Technologies (USA) with the following sequence: 5'-(HS)-GAGGAGTTGGGGGAGCACATT-3'. The oligonucleotide solutions were prepared in sodium phosphate buffer (0.1 $mol.L^{-1}$, pH 7.4) and SSC buffer (sodium chloride 0.3 $mol.L^{-1}$, sodium citrate 0.03 $mol.L^{-1}$, Sigma-Aldrich, USA, pH 7.0) for the electrochemical and optical assays, respectively. Oligonucleotide samples were stored at -8 °C.

2.2 Apparatus

The electrochemical studies were conducted in a potentiostat from CH Instruments 620C and Autolab PGSTAT 302N potentiostat/galvanostat with a FRA2 module. A three-electrode electrochemical cell was employed for the electrochemical experiments. A gold electrode (2 mm diameter, CH Instruments) was used as working electrode, a platinum wire as auxiliary electrode, and Ag/AgCl (KCl 3.0 $mol.L^{-1}$) as a reference electrode. The assays using AuNPs were carried out using a Shimadzu UV-1650PC spectrophotometer. The surface morphology was assessed with an atomic force microscopy (SPM 9600 Shimadzu).

2.3 Preparation of the gold electrode modified with rGO

Gold electrodes (Au) were initially sonicated with ethanol (70%) for 10 minutes, mechanically polished with alumina slurry (0.3 μm) and washed with deionized water and dried in the air. The preconditioning of the electrode was performed in a 0.5 $mol.L^{-1}$ H_2SO_4 (98%, Synth) solution through cyclic voltammetry between +0.0 V and +1.2 V, 5 cycles, 50 $mV.s^{-1}$. Graphene oxide was produced according to the Hummers method [26], and then reduced with hydrazine (64%, Dynamic) [27]. An aqueous dispersion of the reduced graphene oxide (rGO, 6 μL, 1 $mg.mL^{-1}$) was applied to the surface of the gold electrode and maintained at 55 °C until complete drying. The washing of the gold electrode modified with rGO was performed by immersion in phosphate buffer for 15 seconds.

2.4 Genomic DNA samples

Genomic DNA of HBV-positive or negative patients were provided by the Adolfo Lutz Institute (Ethics Committee number 1.131.34). For the selectivity tests, *E. coli* genomic DNA, hepatitis C virus (HCV) genomic RNA and health plasma samples (HS) were used. The genomic DNA was extracted with an ABBOTT m2000sp extractor, and DNAse free water was used in the elution buffer. The health plasma samples were obtained from the Clinical Hospital of the Federal University of Uberlândia. These samples were incubed with a lysis buffer (EDTA 25 $mmol.L^{-1}$, Tris-HCl 200 $mmol.L^{-1}$, NaCl 250 $mmol.L^{-1}$, SDS 1%, pH = 7.5) for 1 hour at 25ºC prior to its use. The genomic DNA was diluted (1:100) in phosphate buffer for electrochemical tests and in SSC buffer for the optical assays. All genomic DNA samples were submitted to thermal denaturation at 98 ºC for 5 minutes before hybridization to obtain the single-stranded DNA (ssDNA).

2.5 Genosensor construction

3 μL of HEPB1S probe ($1x10^{-6}$ $mol.L^{-1}$) were added onto the surface of the gold electrode modified with rGO (Au/rGO). Then, 4 μL of sodium sulfate dodecyl solution (0.1 $mol.L^{-1}$) were applied for 5 minutes, at room temperature, to remove non-adsorbed HEPB1S probe. For the surface blocking of the modified electrode, bovine serum albumin solution (4 μL, 0.5% w/v) was applied and then incubated for 30 minutes at 37 °C. The washing of the gold electrode modified with rGO and sensibilized with HEPB1S was performed by immersion in phosphate buffer for 15 seconds.

2.6 Electrochemical detection by the genosensor

5 μL of positive or negative genomic DNA samples were applied on the surface of the genosensor, maintened for 20 minutes at 55 °C and then washed with phosphate buffer solution. For the detection, ethidium bromide solution (4 μL, $1x10^{-4}$ $mol.L^{-1}$) was applied onto the electrode, then incubated for 10 minutes at room temperature and washed with deionized water. Differential pulse voltammetry measurements were conducted in phosphate buffer as electrolyte.

To calibration curve construction, HepB gDNA samples (0.00765 ng.μL^{-1}, 0.0765 ng.μL^{-1}, 0. 765 ng.μL^{-1}, 7.65 ng.μL^{-1}) were added to the biosensor and maintained at 55 ºC for 30 minutes. For the detection, phosphate buffer, pH 7.4, was used as electrolyte. Data are representative of three independent experiments and values are expressed in mean ± standard deviation.

The measurements of the electrochemical impedance spectroscopy (*EIS*) was performed at perturbation amplitude of 10 mV and frequency range of 10 kHz to 0.1 Hz in 5.00 mmol.L^{-1} $K_4Fe(CN)_6/K_3Fe(CN)_6$ containing 0.10 mol.L^{-1} KCl solution.

2.7 Assay using gold nanoparticles (AuNPs)

The AuNPs were produced using a modified Turkevich-Frens method [28]. In this method, gold salts are reduced, which leads to the nucleation and growth of gold nanoparticles with 15 to 20 nm in size, stabilized by citrate ions. After synthesis, the AuNPs were stored at 4 °C until use. 2 µL of the probe solution (HEPB1S, 126 µmol.L^{-1}) were conjugated with 200 µL of AuNps solution and maintained at room temperature for 1 hour. Microtubes containing the modified AuNPs with HEPB1S were submited to 98 °C for 5 minutes. Then, 2 µL of the HBV genomic DNA (1:100) were added and maintained at 55 °C for 20 min for the duplex formation. Prior to the hybridization process, the genomic DNA was digested using the restriction enzyme EcoRI, which was diluted in a specific buffer (50 mmol.L^{-1} NaCl, 10 mmol.L^{-1} Tris-HCl, 10 mmol.L^{-1} $MgCl_2$, DTT 1 mmol.L^{-1}, pH 7.6). Saturated sodium chloride solution was used to promote the aggregation of AuNPs. Absorbance measurements were monitored by UV-VIS spectroscopy.

3 Results and Discussion

3.1 Electrochemical impedance spectroscopy analysis

The Electrochemical Impedance Spectroscopy (*EIS*) spectra were plotted in the form of Nyquist plots (Fig. 2A and 2B) and fitted to obtain the theoretical curve corresponding to the equivalent circuit with frequency response (NOVA 1.0). Electrochemical impedimetric measurements were recorded using Au, Au/rGO/HEPB1S probe, Au/rGO/HEPB1S:positive sample (HBV genomic DNA) and

Au/rGO/HEPB1S:negative sample (*E. coli* genomic DNA, HCV genomic RNA and healthy plasma samples).

Here Figure 2

Bare gold presents a very small semicircle domain, indicating a low electron-transfer resistance (*Rct*= 300Ω), Fig. 2A (curve a). For Au/rGO (Fig. 2A, curve b) there was the absence of the semicircle caused by the increase in electrical conductivity of the nanocomposite (see inset) when compared to the bare Au.

In the current literature are not found any studies about the force that keeps the reduced graphene oxide sticking onto gold, but it is known that this structure is a derived of graphene oxide that has functional groups containing oxygen removed, in order to make it more similar to graphene. Graphene films supported by metal substrates generally display charge transfer with the metal surface [29]. Specifically, charge transfer from graphene to gold has been observed, resulting in a slight p-type doping of the graphene [30-34], with a binding energy between graphene and gold smaller than 40 meV per C atom [30-32].

After the biofunctionalization steps, Au/rGO/HEPB1S probe (Fig. 2B, curve b) showed an increase in the charge transfer resistance (*Rct*= 723 Ω), indicating that hepB1S was immobilizated onto Au/rGO.

Reduced graphene oxide (rGO), produced by reduction of graphene oxide with hydrazine, contains oxygen functional groups, including hydroxyl and carboxyl groups as well as hydrazone groups (R_2C=N-NH_2), resulting from the reduction of carbonyl functions [35]. These organic functions enable interaction of the rGO with DNA by hydrogen bonds. rGO structure is also formed by carbon-rich regions, containing condensed aromatic rings, which can bind to the aromatic rings of DNA bases through π-π stacking, favoring DNA adsorption [36]. Still, scanning electron microscopy (SEM) images of a gold surface unmodified or modified with rGO shows that, after modification with rGO, the material is well distributed over almost the entire electrode surface, indicating good coverage, but does not cover all the electrode surface (results not shown). In conclusion, it is possible to graft the DNA onto the rGO-Au electrode through π-π stacking, as well as by hydrogen and covalent (S-Au) bonds.

After the addition of the genomic DNA (sample positive), an increase of about 2.5 times in the charge transfer resistance values was observed (*Rct*= 1721Ω), Fig 2B, curve d. The addition of the negative control (*Rct* = 817Ω), does not cause a substantial difference in the resistance (Fig 2B, curves a and c) when compared to the Au/rGO/HEPB1S probe response (Fig. 2B, curve b).

The increase in diameter of the semicircles observed after hybridization is due to the adsorption of biomolecules, which retards the electron transfer kinetics between the redox probe and the electrode surface [37] and shows that the genosensor is capable of discriminating specific or non-specific samples. Rct values of the samples of HBV-positive patients were higher in relation to the negative samples demonstrating the selectivity of the interaction of the probe with the HBV genomic DNA. The response of the system was presented using the Δ*ratio* (Fig. 2C) described in previous studies [38].

Δ*ratio* = ΔHBV genomic DNA /Δ HEPB1S
Δ HBV genomic DNA = *Rct* (HEPB1S: HBV genomic ssDNA)
Δ HEPB1S = *Rct* (probe)

Where *Rct* (probe) is the charge transfer resistance value obtained after the probe immobilization on the electrode, and Rct (HEPB1S: HBV genomic ssDNA) is the charge transfer resistance value observed after the incubation with the target analyte genomic ssDNA. The reproducibility of obtained results was evaluated using three electrodes.

Images of the bare Au electrode, Au/rGO, Au/rGO/HEPB1S/BSA, Au/rGO/HEPB1S/BSA/HBV genomic DNA (target) and Au/rGO/HEPB1S/ BSA/*E. coli* genomic DNA (NC) presented roughness values (*Rq*) of 14 ± 1.20 nm, 185 ± 12.60 nm, 97 ± 1.22 nm, 226.2 ± 10.29 nm and 135 ± 8.29 nm, respectively. After the probe immobilization, there was a decrease of 47.5% in *Rq* values, and in the presence of the target there was a significantly increase, possibly due to the structure of the genomic DNA, more elongated and less flexible than is the probe [24, 39, 40]. These results showed that there was the duplex formation (double-stranded DNA), in accordance with electrochemical and optical studies. AFM images corroborate with the results obtained by *EIS*, since that the increase in the charge transfer resistance (*Rct*) values is according to the increase in the roughness (*Rq*) values for the surfaces evaluated. Rougher surfaces

cause a decrease in the charge permeability of the Au/rGO/HEPB1S/BSA/HBV genomic DNA to a redox probe, increasing the *Rct* values.

3.2 Detection by differential pulse voltammetry

DNA hybridization events can be monitored through indirect detection using redox indicators, such as ethidium bromide intercalator [24, 41].

Figure 3 shows the differential pulse voltammogram relative to the oxidation of ethidium bromide using genomic DNA.

Here Figure 3

It can be observed that the oxidation peak of ethidium bromide occurs at +0.6 V. When the treated healthy plasma samples were added to the genosensor (rGO/gold electrode/HEPB1Sprobe), the current values observed were similar to those of the probe. However, with the addition of HBV genomic DNA (*i*p = 4.09 μA ± 0.19 μA), an increase of about 1.4 times was observed when compared to the probe (*ip* = 2.93 μA ± 0.24 μA), indicating accumulation of the ethidium bromide on the surface of the genosensor and duplex formation (Fig. 3A).

In Fig. 3B, we observed a linear relationship with log [HepB gDNA] given by ΔQ = 13.99 + 2.34 log [HepB gDNA], being R= 0.997. The electrochemical biosensor detected until 7.65 pg.μL^{-1}.

The histogram (Fig. 3C) shows the bar chart charge resultant of the oxidation process of the ethidium bromide for positive and negative samples for HBV. We observed an increase in the charge values after the incubation with the positive sample for the HBV, evidencing the specificity of the probe, which was able to differentiate the positive samples from the negative samples (for example, HCV) obtained from the patients with hepatitis B. The concentrations of HBV positive samples determined using the calibration curve data were: 0.70 ng.μL^{-1} (1); 1.86 ng.μL^{-1} (2); 102.10 ng.μL^{-1} (3); 0.20 ng.μL^{-1} (4), 0.45 ng.μL^{-1} (5), 29.38 ng.μL^{-1} (6); 1.83 ng.μL^{-1} (7); 12.67 ng.μL^{-1} (8); 0.253 ng.μL^{-1} (9); 0.87 ng.μL^{-1} (10).

3.3 Analysis using AuNPs

The AuNP synthesis and the catalytic properties of AuNPs have been employed to develop colorimetric sensors [42]. Colorimetric assays and ultraviolet-visible spectrophotometry (UV-vis) using AuNPs sensibilizated with HEPB1S in the presence or absence of samples positive or negative for the Hepatitis B, genomic DNA or blood plasma, were carried out (Figs. 4 and 5). The color change of AuNP conjugated with the specific probe represents promising sensor platforms for disease diagnosis [43-45]. Images of colorimetric transition for the system containing: AuNP, AuNP/HEPB1S, AuNP/HEPB1S/positive sample, AuNP/HEPB1S/negative samples and AuNP saturated sodium chloride solution (blank) is shown in the Figure 4.

Here Figure 4

Considering that gold has affinity with compounds containing sulfur atoms [46] the conjugation of the probe HEPB1S was facilitated, and it maintained the AuNPs stabilized, as the absorbance peak remained close to 520 nm.

AuNPs are highly dependent on the ionic strength solution. In the presence of saturated NaCl solution, Au-NPs are destabilized due to the alteration of the ionic force, which disrupts the citrate ion network located around the nanoparticles (Fig. 4B, curve e).

After sensibilization of the AuNP with probe DNA (HEPB1S), no alteration was observed in the color of coloidal suspension. Adding target (HBV-positive samples) caused color change (light red to blue) due to the aggregation of the nanoparticles and interaction with the HepB1 probe: HBV genomic DNA, and a shift of the absorption band to longer wavelengths, between 540 - 590 nm (Fig. 4B). The red-shift of the peak wavelength was linearly proportional to the concentration of HBV-genomic DNA from 1.55 to 6.68 ng/μL^{-1} with a detection limit of 0.15 ng.μL^{-1} (N = 3, R = 0.98) and sensitivity of 9.1 nm/ng.μL^{-1} (Fig. 4C).

Works aiming the development of colorimetric and optical biosensors for HBV using nanoparticles as platform and specific antigen or DNA as probe are described in the literature [25, 47-50]. Xi and collaborators using gold nanoparticle grafted onto nylon membrane [48] and gold-coated iron oxide nanoparticles [49] developed a

colorimetric system with detection limits of $1x10^{-11}$ mol/L and $1x10^{-16}$ mol/L, respectively. Another colorimetric assay with HBV-specific oligonucleotides as a probe using silver-coated glass and DNAzyme G-quadruplex-hemin, obtained a linear response range of 0.5 nmol/L to 100 nmol/L with a detection limit of 0.2 nmol/L [50]. Mao *et al.* [22] developed a colorimetric method based in copper nanoclusters for the HBV-DNA with limit of detection of 12×10^9 molecules.

In the present work, the detection limit of 0.15 ng.µL^{-1} (0.721 pmol/L or 9 x 10^6 copies/µL, HBV genome = 3.2 Kbp), indicates that the biosensor is promising. Still, the AuNps/HEPB1S system was effective in detecting the HBV genomic DNA discriminating HBV-negative samples in blood plasma.

In order to verify the applicability of the sensor for clinical samples, tests were performed in blood plasma with success (Figure 5).

Here Figure 5

For the analysis conducted in blood plasma, that is rich in interfering substances (proteins, amino acids, uric acid, ascorbic acid and others), the genosensor was specific since that, further of the color change, a bathochromic shift (146 nm) was observed using positive HBV samples (Fig. 5d), while for the negative control (Fig. 5c) occurs a small bathochromic shift (19 nm) and no color change when compared to AuNPs/Hep1S (Fig 5b). The system was able to discriminate efficiently healthy or sick patients, being able be applied in real samples without prior purification.

4 Conclusion

This work proposed four techniques for the detection of the hepatitis B virus in biological samples. The specificity of the HBV probe can be confirmed by voltammetry, impedance spectroscopy, absorbance measurements and AFM images. VPD and *EIS* for the genosensors demonstrated significant advantages in terms of response with the positive target addition, since HBV positive samples result in a change of about 1.4-fold and 2-fold compared to the negative samples.

Assays using the electrochemical biosensor or coloidal suspension of gold nanoparticules detected until 7.65 pg.µL^{-1} or 0.15 ng.µL$^{-1,}$ respectively, of the HBV-target indicating better sensibility for the electrochemical biosensor.

The produced genosensors enabled the discrimination of hepatitis B and hepatitis C. This assay presents promising results for the selective detection of hepatitis B in biological samples.

Acknowledgements

The authors are grateful for the financial support from Conselho Nacional de Desenvolvimento Científico e Tecnológico (CNPq), Fundação de Amparo à Pesquisa do Estado de Minas Gerais (FAPEMIG) and Coordenação de Aperfeiçoamento de Pessoal de Nível Superior (CAPES). Also, we would like to thank teacher Abílio Borghi for the review of the English manuscript.

Figure captions

Figure 1. Schematic illustration of the manufacturing steps of the DNA sensors.

Figure 2. Nyquist plots in $K_4Fe(CN)_6/K_3Fe(CN)_6$ redox pair for: (**A**) bare gold electrode (a) and Au/rGO electrode (b). (**B**) Au/rGO/HEPB1S/HCV genomic RNA (a), Au/rGO/HEPB1S (b), Au/rGO/HEPB1S/*E. coli* genomic DNA (c), Au/rGO/HEPB1S/positive sample (d). Inset: equivalent circuit, where, *Rs*, *RW*, *Rct* and CPE represent the solution resistance, the Warburg diffusion resistance, the charge-transfer resistance and the constant phase element, respectively. (**C**) Histogram showing the Δ*ratio* for the positive (1-6) or negative samples (*E. coli*, HCV, HS1 and HS2). The AFM images for the evaluated surfaces are indicated in A and B.

Figure 3. (**A**) Differential pulse voltammograms (baseline subtracted) of the ethidium bromide oxidation onto transducer surface: in absence (a) or presence: healthy plasma (b) and HBV positive sample (c). (**B**) Relation between charge and log [Hep B gDNA], N=3. (**C**) Histogram obtained from differential pulse voltammograms in the absence (probe) or presence of *E. coli* genomic DNA, HCV genomic RNA, healthy plasma samples (HS1 and HS2) and the genomic DNA samples of ten positive patients for HBV (1-10). Supporting electrolyte: phosphate buffer (0.10 $mol.L^{-1}$, pH 7.4), modulation amplitude: 25 mV, pulse interval: 0.2 s, scan rate: 30 $mV.s^{-1}$.

.

Figure 4. (**A**) Photographs of microtubes showing color formation for samples: AuNPs, AuNPs/HEPB1S, AuNPs/HEPB1S/*E. coli* (EC), AuNPs/HEPB1S/HCV genomic RNA (HCV), AuNPs/HEPB1S/healthy plasma samples 1 and 2 (HS1 and HS2) and AuNPs/NaCl saturated solution (blank). Samples (1-10): AuNPs/HEPB1S/HBV positive samples. (**B**) Absorption spectrum for: AuNPs (a), AuNPs/HEPB1S (b), AuNPs/HEPB1S/positive sample (c), AuNPs/HEPB1S/ *E. coli* genomic DNA (d) and AuNPs/ NaCl saturated solution (blank) (e). **(C)**. Calibration curve for the spectrophotometric determination of HBV.

FIGURE 5. Images and absorption spectra in UV-VIS using blood plasma of four patients. AuNPs with NaCl (a), AuNPs/Hep1S with NaCl (b), AuNPs/Hep1S/plasma from healthy patients (negative control) with NaCl (c), AuNPs/Hep1S/plasma from sick patients (positive control) with NaCl (d).

References

[1] S. Hajihosseini, N. Nasirizadeh, M.S. Hejazi, P. Yaghmaei, A sensitive DNA biosensor fabricated from gold nanoparticles and graphene oxide on a glassy carbon electrode, Mater Sci Eng C Mater Biol Appl. 61 (2016) 506-515.

[2] H. Kazerooni, B. Nassernejad, A novel biosensor nanomaterial for the ultraselective and ultrasensitive electrochemical diagnosis of the breast cancer-related BRCA1 gene, Anal Methods-Uk 8 (2016) 3069-3074.

[3] N.T. Shelke, B.R. Karche, Ultraviolet photosensor based on few layered reduced graphene oxide nanosheets, Appl. Surf. Sci. 418 (2017) 374-379.

[4] V.S.A. Piriya, P. Joseph, S.C.G.K. Daniel, S. Lakshmanan, T. Kinoshita, S. Muthusamy, Colorimetric sensors for rapid detection of various analytes, Mater. Sci. Eng. C Mater. Biol. Appl. 78 (2017) 1231-1245.

[5] Y.H. Wang, H.H. Deng, Y.H. Liu, X.Q. Shi, A.L. Liu, H.P. Peng, G.L. Hong, W. Chen, Partially reduced graphene oxide as highly efficient DNA nanoprobe, Biosens. Bioelectron. 80 (2016) 140-145.

[6] J.V. da Silva, A.G.B. Madurro, J.M. Madurro, Modified electrode with reduced graphene oxide/poly(3-hydroxyphenylacetic acid): a new platform for oligonucleotide hybridization, J. Solid State Electr. 21(7) (2017) 2129-2139

[7] A.M. Baetsen-Young, M. Vasher, L.L. Matta, P. Colgan, E.C. Alocilja, B. Day, Direct colorimetric detection of unamplified pathogen DNA by dextrin-capped gold nanoparticles, Biosens. Bioelectron. 101 (2018) 29-36.

[8] W.Q. Wei, Q. Feng, L. Jiang, M.S. Waitara, O.F. Iwuchukwu, D.M. Roden, M. Jiang, H. Xu, R.M. Krauss, J.I. Rotter, D.A. Nickerson, R.L. Davis, R.L. Berg, P.L. Peissig, C.A. McCarty, R.A. Wilke, J.C. Denny, Characterization of statin dose response in electronic medical records, Clin. Pharmacol. Ther. 95 (2014) 331-338.

[9] L. Hlavata, K. Benikova, V. Vyskocil, J. Labuda, Evaluation of damage to DNA induced by UV-C radiation and chemical agents using electrochemical biosensor based on low molecular weight DNA and screen-printed carbon electrode, Electrochim. Acta 71 (2012) 134-139.

[10] H. Ravan, S. Kashanian, N. Sanadgol, A. Badoei-Dalfard, Z. Karami, Strategies for optimizing DNA hybridization on surfaces, Anal. Biochem. 444 (2014) 41-46.

[11] E. Paleček, Oscillographic Polarography of Highly Polymerized Deoxyribonucleic Acid, Nature 188 (1960) 656–657.

[12] T.G. Drummond, M.G. Hill, J.K. Barton, Electrochemical DNA sensors, Nat. Biotechnol. 21 (2003) 1192-1199.

[13] Y.H. Choi, G.Y. Lee, H. Ko, Y.W. Chang, M.J. Kang, J.C. Pyun, Development of SPR biosensor for the detection of human hepatitis B virus using plasma-treated parylene-N film, Biosens. Bioelectron. 56 (2014) 286-294.

[14] C.C. Chen, Z.L. Lai, G.J. Wang, C.Y. Wu, Polymerase chain reaction-free detection of hepatitis B virus DNA using a nanostructured impedance biosensor, Biosens. Bioelectron. 77 (2016) 603-608.

[15] T. Riedel, F. Surman, S. Hageneder, O. Pop-Georgievski, C. Noehammer, M. Hofner, E. Brynda, C. Rodriguez-Emmenegger, J. Dostalek, Hepatitis B plasmonic

biosensor for the analysis of clinical serum samples, Biosens. Bioelectron. 85 (2016) 272-279.

[16] M.H. Mashhadizadeh, R.P. Talemi, Synergistic effect of magnetite and gold nanoparticles onto the response of a label-free impedimetric hepatitis B virus DNA biosensor, Mater. Sci. Eng. C Mater. Biol. Appl. 59 (2016) 773-781.

[17] H. Xu, D. Gu, J. He, L. Shi, J. Yao, C. Liu, C. Zhao, Y. Xu, S. Jiang, J. Long, Multiplex biomarker analysis biosensor for detection of hepatitis B virus, Biomed. Mater. Eng. 26 Suppl 1 (2015) S2091-2100.

[18] Z. Shakoori, S. Salimian, S. Kharrazi, M. Adabi, R. Saber, Electrochemical DNA biosensor based on gold nanorods for detecting hepatitis B virus, Anal. Bioanal. Chem. 407 (2015) 455-461.

[19] V.C. Diculescu, A.-M. Chiorcea-Paquim, A.M. Oliveira-Brett, Applications of a DNA-electrochemical biosensor, Trends. Analyt. Chem. 79 (2016) 23-36.

[20] C.C. Chen, Z.L. Lai, G.J. Wang, C.Y. Wu, Polymerase chain reaction-free detection of hepatitis B virus DNA using a nanostructured impedance biosensor, Biosens. Bioelectron. 77 (2016) 603-608.

[21] L.E. Ahangar, M.A. Mehrgardi, Amplified detection of hepatitis B virus using an electrochemical DNA biosensor on a nanoporous gold platform, Bioelectrochemistry 117 (2017) 83-88.

[22] X. Mao, S. Liu, C. Yang, F. Liu, K. Wang, G. Chen, Colorimetric detection of hepatitis B virus (HBV) DNA based on DNA-templated copper nanoclusters, Anal. Chim. Acta 909 (2016) 101-108.

[23] L. Yang, M. Li, F. Du, G. Chen, A. Yasmeen, Z. Tang, A Novel Colorimetric PCR-Based Biosensor for Detection and Quantification of Hepatitis B Virus, Methods Mol. Biol. 1571 (2017) 357-369.

[24] A.C.H. Castro, E.G. Franca, L.F. de Paula, M.M.C.N. Soares, L.R. Goulart, J.M. Madurro, A.G. Brito-Madurro, Preparation of genosensor for detection of specific DNA sequence of the hepatitis B virus, Appl. Surf. Sci. 314 (2014) 273-279.

[25] C.C. Chen, Z.L. Lai, G.J. Wang, C.Y. Wu, Polymerase chain reaction-free detection of hepatitis B virus DNA using a nanostructured impedance biosensor, Biosens. Bioelectron. 77 (2016) 603-608.

[26] W.S. Hummers, R.E. Offeman, Preparation of Graphitic Oxide, J. Am. Chem. Soc. 80 (1958) 1339-1339.

[27] H.W. Wang, Z.A. Hu, Y.Q. Chang, Y.L. Chen, Z.Y. Zhang, Y.Y. Yang, H.Y. Wu, Preparation of reduced graphene oxide/cobalt oxide composites and their enhanced capacitive behaviors by homogeneous incorporation of reduced graphene oxide sheets in cobalt oxide matrix, Mater. Chem. Phys. 130 (2011) 672-679.

[28] G. Frens, Controlled Nucleation for the Regulation of the Particle Size in Monodisperse Gold Suspensions, Nature 241 (1973) 20-22.

[29] J.M. Wofford, E. Starodub, A.L Walter, S. Nie, A. Bostwick, N.C. Bartelt, K. Thurmer, E. Rotenberg, K.F. McCarty, O.D. Dubon, Extraordinary epitaxial alignment of graphene islands on Au(111), New Journal of Physics 14 (2012) 053008.

[30] S. Nie, N.C. Bartelt, J.M. Wofford, O.D. Dubon, K.F. McCarty, K. Thürmer. Scanning tunneling microscopy study of graphene on Au(111): Growth mechanisms and substrate interactions. Phys. Rev. B 85 (2012) 205406

[31] G. Giovannetti, P. A. Khomyakov, G. Brocks, V.M. Karpan, J. van den Brink, P.J. Kelly, Doping graphene with metal contacts. Phys. Rev. Lett. 101 (2008) 026803.

[32] M. Vanin, J.J. Mortensen, A.K. Kelkkanen, J.M. Garcia-Lastra, K.S. Thygesen, K.W. Jacobsen, Graphene on metals: A van der Waals density functional study, Phys. Rev. B 81 (2010) 081408.

[33] A. Varykhalov, M.R. Scholz, T.K. Kim, O. Rader, Effect of noble-metal contacts on doping and band gap of graphene. Phys. Rev. B 82 (2010) 121101.

[34] Z. Klusek, P. Dabrowski, P. Kowalczyk, W. Kozlowski, W. Olejniczak, P. Blake, M. Szybowicz, T. Runka, Graphene on gold: Electron density of states studies by scanning tunneling spectroscopy Appl. Phys. Lett. 95 (2009) 113114.

[35] C.K. Chua, M. Pumera, The reduction of graphene oxide with hydrazine: Elucidating its reductive capability based on reaction-model approach, Chem. Commun. 52 (2016) 72-75.

[36] C. Lu, P.J. Huang, B. Liu, Y. Ying, J. Liu, Comparison of Graphene Oxide and Reduced Graphene Oxide for DNA Adsorption and Sensing. Langmuir 32 (2016) 10776−10783.

[37] D.E. Souto, J.V. Silva, H.R. Martins, A.B. Reis, R.C. Luz, L.T. Kubota, F.S. Damos, Development of a label-free immunosensor based on surface plasmon resonance technique for the detection of anti-Leishmania infantum antibodies in canine serum, Biosens. Bioelectron. 46 (2013) 22-29.

[38] A. Bonanni, M.J. Esplandiu, M.I. Pividori, S. Alegret, M. del Valle, Impedimetric genosensors for the detection of DNA hybridization, Anal. Bioanal. Chem. 385 (2006) 1195-1201.

[39] A.M. Oliveira-Brett, J.A.P. Piedade, L.A. Silva, V.C. Diculescu, Voltammetric determination of all DNA nucleotides, Anal. Biochem. 332 (2004) 321-329.

[40] R.P.A. Balvedi, A.C.H. Castro, J.M. Madurro, A.G. Brito-Madurro, Detection of a Specific Biomarker for Epstein-Barr Virus Using a Polymer-Based Genosensor, Int. J. Mol. Sci. 15 (2014) 9051-9066.

[41] S.H. Minasyan, L.A. Tavadyan, A.P. Antonyan, H.G. Davtyan, M.A. Parsadanyan, P.O. Vardevanyan, Differential pulse voltammetric studies of ethidium bromide binding to DNA, Bioelectrochemistry 68 (2006) 48-55.

[42] W.W. Chen, Y.M. Guo, W.S. Zheng, Y.L. Xianyu, Z. Wang, X.Y. Jiang, Recent Progress of Colorimetric Assays Based on Gold Nanoparticles for Biomolecules, Chinese. J. Anal. Chem. 42 (2014) 307-314.

[43] S.S. Agasti, S. Rana, M.H. Park, C.K. Kim, C.C. You, V.M. Rotello, Nanoparticles for detection and diagnosis, Adv. Drug. Deliv. Ver. 62 (2010) 316-328.

[44] M. Cordeiro, F. Ferreira Carlos, P. Pedrosa, A. Lopez, P.V. Baptista, Gold Nanoparticles for Diagnostics: Advances towards Points of Care, Diagnostics 6 (2016) 43.

[45] L.M. Alves, V.R. Rodovalho, A.C.H. Castro, M.A.R. Freitas, C.M. Mota, T.W.P. Mineo, J.R. Mineo, J.M. Madurro, A.G. Brito-Madurro, Development of direct assays for Toxoplasma gondii and its use in genomic DNA sample, J. Pharm. Biomed. Anal. 145 (2017) 838-844.

[46] A.A.S. Oliveira, D.A.S. Costa, I.F. Teixeira, F.C.C. Moura, Gold nanoparticles supported on modified red mud for biphasic oxidation of sulfur compounds: A synergistic effect, Appl. Catal. B Environ. 162 (2015) 475-482.

[47] M. Shevtsov, L. Zhao, U. Protzer, M. Klundert, Applicability of Metal Nanoparticles in the Detection and Monitoring of Hepatitis B Virus Infection, Viruses. 9 (2017) 193.

[48] D. Xi, X. Luo, Q. Ning, Q. Lu, K. Yao, Z. Liu, The detection of HBV DNA with gold nanoparticle gene probes, J. Nanjing Med. Univ. 21 (2007) 207–212.

[49] D. Xi, X. Luo, Q. Lu, K. Yao, Z. Liu, Q. Ning, The detection of HBV DNA with gold-coated iron oxide nanoparticle gene probes, J. Nanoparticle Res. 10 (2008) 393–400.

[50] Y. Li, S. Liu, Q. Deng, L. Ling, A sensitive colorimetric DNA biosensor for specific detection of the HBV gene based on silver-coated glass slide and G-quadruplex-hemin DNAzyme, J. Med. Virol. 90 (2018) 699–705.

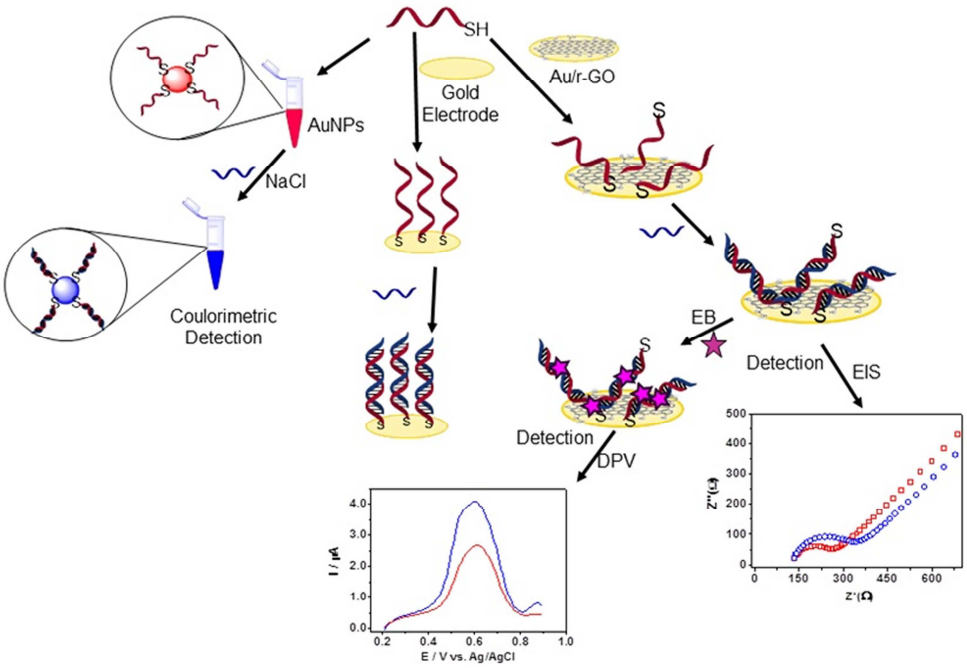

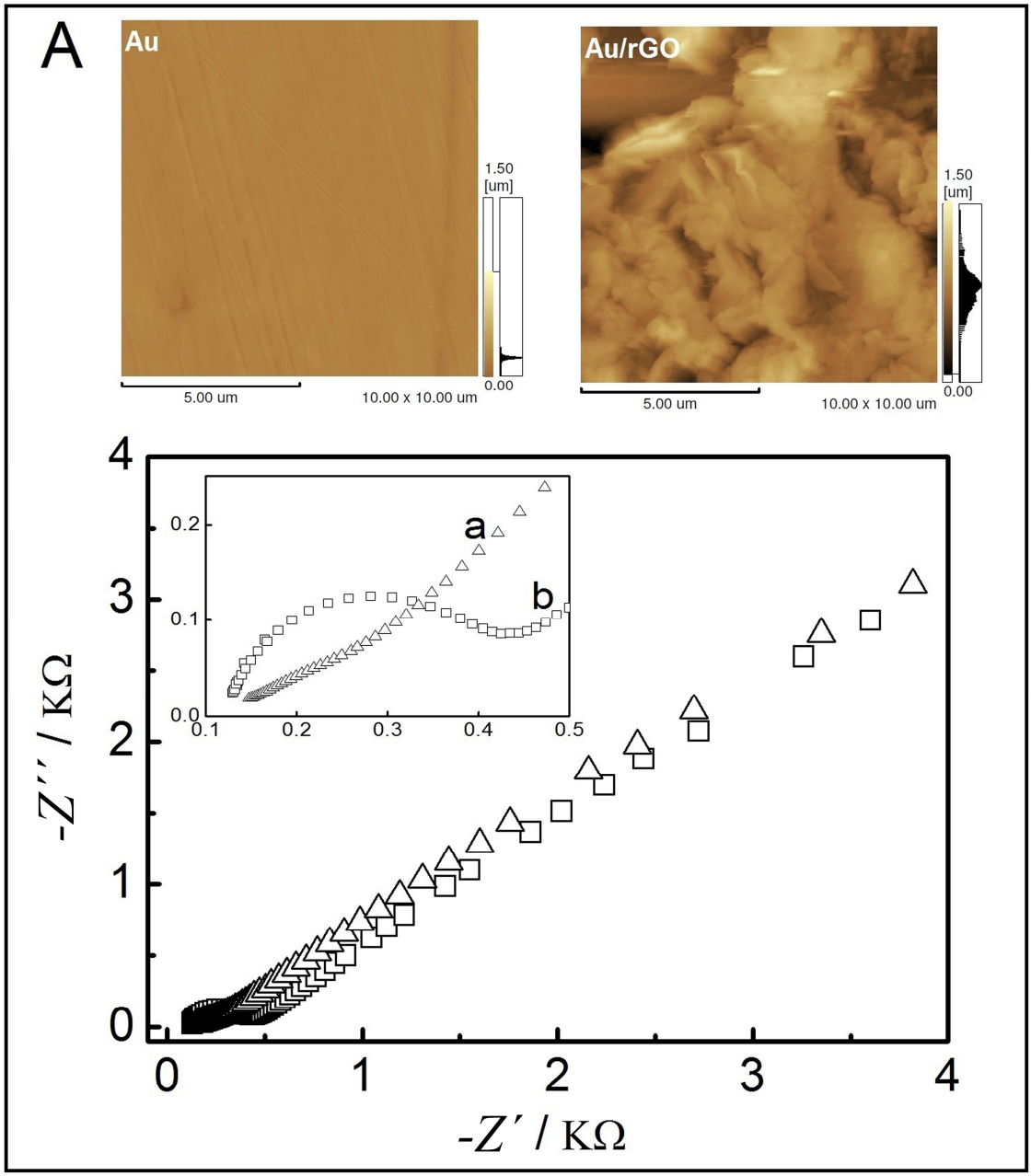
A
Au
1.50
[um]
0.00
5.00 um
10.00 x 10.00 um
Au/rGO
1.50
[um]
0.00
5.00 um
10.00 x 10.00 um
-Z'' / KΩ
-Z' / KΩ
a
b
0
1
2
3
4
0.0
0.1
0.2
0.3
0.4
0.5